





ORIGINAL RESEARCH

Fractional Flow Reserve and Instantaneous Wave-Free Ratio Predict Pathological Wall Shear Stress in Coronary Arteries: Implications for Understanding the Pathophysiological Impact of Functionally Significant Coronary Stenoses

Christopher C. Y. Wong, MPhil; Ashkan Javadzadegan, PhD; Cuneyt Ada , MBBS; Jerrett K. Lau, PhD; Ravinay Bhindi, PhD; William F. Fearon , MD; Leonard Kritharides , PhD; Martin K. C. Ng, PhD; Andy S. C. Yong , PhD

BACKGROUND: The pathophysiological mechanism behind adverse outcomes associated with ischemia-inducing epicardial coronary stenoses and microcirculatory dysfunction remains unclear. Wall shear stress (WSS) plays an important role in atherosclerotic plaque progression and vulnerability. We aimed to evaluate the relationship between WSS, functionally significant epicardial coronary stenoses, and microcirculatory dysfunction.

METHODS AND RESULTS: Patients undergoing invasive coronary physiology testing were included. Fractional flow reserve, instantaneous wave-free ratio, and the index of microcirculatory resistance were measured. Quantitative coronary angiography was used to obtain the lesion percentage diameter stenosis. Computational fluid dynamics analysis was performed to calculate WSS parameters. Multiple regression analysis was performed to calculate the standardized regression coefficient (β) for the coronary physiology indices.

A total of 107 vessels from 88 patients were included. Fractional flow reserve independently predicted the total area of low WSS ($\beta=-0.44$; 95% CI, -0.62 to -0.25 ; $P<0.001$) and maximum lesion WSS ($\beta=-0.53$; 95% CI, -0.70 to -0.36 ; $P<0.001$) after adjusting for percentage diameter stenosis and index of microcirculatory resistance. Similarly, instantaneous wave-free ratio also independently predicted the total area of low WSS ($\beta=-0.45$; 95% CI, -0.62 to -0.28 ; $P<0.001$) and maximum lesion WSS ($\beta=-0.58$; 95% CI, -0.73 to -0.43 ; $P<0.001$). The index of microcirculatory resistance did not predict either low or high WSS.

CONCLUSIONS: Fractional flow reserve and instantaneous wave-free ratio independently predicted the total burden of low WSS and maximum lesion WSS in coronary arteries. No relationship was found between microcirculatory dysfunction and WSS.

Key Words: fractional flow reserve ■ index of microcirculatory resistance ■ instantaneous wave-free ratio ■ wall shear stress

Myocardial ischemia has long been associated with poor outcomes in patients with coronary artery disease.¹ Studies have established fractional flow reserve (FFR) as a more important

prognosticator than angiographic severity in patients undergoing revascularization.^{2,3} Coronary microvascular dysfunction, defined by abnormal index of microcirculatory resistance (IMR), is also associated

Correspondence to: Andy S. C. Yong, PhD, Department of Cardiology, Level 3 West, Concord Hospital, Concord Road, NSW 2139, Australia.
E-mail: andy.yong@sydney.edu.au

For Sources of Funding and Disclosures, see page 10.

© 2022 The Authors. Published on behalf of the American Heart Association, Inc., by Wiley. This is an open access article under the terms of the Creative Commons Attribution-NonCommercial-NoDerivs License, which permits use and distribution in any medium, provided the original work is properly cited, the use is non-commercial and no modifications or adaptations are made.

JAHA is available at: www.ahajournals.org/journal/jaha

CLINICAL PERSPECTIVE

What Is New?

- Abnormal fractional flow reserve and instantaneous wave-free ratio were associated with both pathological low and high wall shear stress in coronary arteries, irrespective of the underlying lesion's angiographic severity.

What Are the Clinical Implications?

- Given the known relationship between pathological wall shear stress and atherosclerosis progression, our results provide a potential explanation for the higher incidence of adverse events in patients with ischemia-inducing epicardial coronary stenoses.

Nonstandard Abbreviations and Acronyms

3-D	3-dimensional
CFD	computational fluid dynamics
%DS	percentage diameter stenosis
FFR	fractional flow reserve
iFR	instantaneous wave-free ratio
IMR	index of microcirculatory resistance
WSS	wall shear stress

with worse outcomes.⁴ Yet, the pathophysiological mechanisms underpinning the poor prognosis in patients with functionally significant coronary epicardial and microcirculatory disease are not well understood.

Wall shear stress (WSS), the tangential force exerted on the endothelium by blood flow, has been implicated as a cause of the uneven distribution of atherosclerotic disease throughout the coronary circulation.⁵ Low WSS is associated with severe endothelial dysfunction, progression of atherosclerotic plaque, constrictive remodeling, and necrotic core development^{5–8}; whereas high WSS predicts plaque transformation and myocardial infarction.^{9,10}

Currently, it is not known how coronary physiology influences WSS, and determining their relationship may yield insights into the pathophysiological basis for the poor prognosis seen in patients with myocardial ischemia. We therefore performed a study to evaluate whether epicardial and microcirculatory physiology indices can predict abnormal WSS perturbations independent of angiographic severity.

METHODS

The data that support the findings of this study are available from the corresponding author on reasonable request.

Study Population

We included patients who underwent comprehensive invasive coronary physiological assessment at 2 tertiary referral hospitals for research purposes. This population consisted of patients from 3 separate studies: the first enrolled patients between April 2008 and October 2010 to derive a method of calculating IMR without the coronary wedge pressure¹¹; the second evaluated patients between March 2015 and March 2017 to determine the effects of remote ischemic preconditioning on the microcirculation¹²; the third included patients between February 2019 and July 2020 to examine the relationship between the coronary epicardial arteries and the microcirculation (Australian New Zealand Clinical Trials Registry ID: ACTRN12619000450112). Exclusion criteria were culprit vessels in acute coronary syndrome, nonculprit vessels <48 hours after acute ST-segment-elevation myocardial infarction, cardiogenic shock, bypass graft to the target vessel, tortuous vessels precluding safe passage of the pressure guidewire, and any contraindication to adenosine administration. The study protocol conformed to the ethical guidelines of the 1975 Declaration of Helsinki, and was approved by the human research ethics review boards of both institutions. Written informed consent was obtained from all participants. C.C.Y.W. and A.S.C.Y. had full access to all the data in the study and take responsibility for their integrity and the data analysis.

Coronary Angiography and Physiology Measurements

Coronary angiography was performed as per standard institutional practice via the radial or femoral route. After diagnostic angiography, a pressure-temperature sensor guidewire (PressureWire X; Abbott Corporation, Chicago, IL) was advanced to the tip of the guiding catheter and equalized to the guide catheter pressure. The guidewire was then advanced to the distal third of the vessel, at least 3 cm downstream from the target lesion. Intracoronary nitroglycerin was administered at a dose of 100 to 200 µg.

The resting mean proximal pressure and distal pressure were recorded. Three boluses of 3 mL room temperature saline were then injected into the coronary artery via the guiding catheter. The transit time of the saline injections was determined using the thermodilution technique, and the average of the 3 resting transit times was recorded as the resting mean transit

time. An intravenous infusion of adenosine (140 µg/kg per minute) was then administered via a large-bore peripheral cannula or femoral venous sheath for a minimum duration of 90 seconds to achieve maximal hyperemia. The hyperemic mean proximal pressure and distal pressure were recorded. Thermodilution curves were then produced in the same manner to determine the hyperemic mean transit time.

All measurements were recorded using the Coroflow system (Coroventis Research AB, Uppsala, Sweden). FFR was calculated as the ratio of hyperemic mean distal pressure/hyperemic mean proximal pressure. The corrected IMR was calculated in all patients using the following formula: $IMR = \text{hyperemic mean proximal pressure} \times \text{hyperemic mean transit time} \times 1.35 \times [\text{hyperemic mean distal pressure} / \text{hyperemic mean aortic pressure}] - 0.32$. In vessels with significant epicardial stenoses, the commonly used simplified formula ($IMR = \text{hyperemic mean distal pressure} \times \text{hyperemic mean transit time}$) can overestimate IMR by neglecting the significant contribution of collateral flow. The corrected IMR formula accounts for the contribution of collateral flow toward IMR calculation without requiring the additional invasive step of obtaining coronary wedge pressure, and has been shown to have excellent correlation and agreement with true IMR.^{4,11,13} Instantaneous wave-free ratio (iFR) was calculated offline using Matlab version R2019B (Mathwork, MA), as previously described.^{14–16} $FFR \leq 0.80$, $iFR \leq 0.89$, and $IMR \geq 25$ were used as the cutoffs for abnormal values.

Quantitative coronary angiography was performed offline, as previously described.¹⁷ Angiographic images with the least foreshortening were used, and analyses were performed during end diastole. The percentage of diameter stenosis (%DS) was measured twice and averaged by a single experienced interventional cardiologist blinded to the coronary physiology indices.

WSS Calculation

The WSS calculation was performed by an independent analyst blinded to the coronary physiology indices. Three-dimensional (3-D) reconstructions of the target vessels were performed using a Leonardo workstation (IC3D; Siemens, Forchheim, Germany). End-diastolic images from 2 orthogonal angiographic views at least 30° apart were selected for reconstruction. Of the 137 available vessels, 30 were excluded because of inadequate image quality for accurate 3-D reconstruction.

Computational fluid dynamics (CFD) analysis was subsequently performed using methods described in our previous studies.^{18,19} In brief, the reconstructed 3-D models were imported into mesh generation software (ANSYS CFX 12.1, PA). The surfaces of the vessels were triangulated with a node distance between 0.01

and 0.02 mm, and a boundary layer mesh with 4 rows and a growth factor of 1.2 was generated.

For the CFD simulation, flow was considered to be 3-D, steady, and turbulent. Blood was modeled as a noncompressible Newtonian fluid with a dynamic viscosity of 0.0035 Pa·s and a density of 1050 kg/m³. Walls were considered rigid, and a no-slip boundary condition was applied. The inlet and outlet boundary conditions were individualized and set to the patients' invasively measured aortic and distal coronary pressure, respectively. The fluid motion equations were solved using the finite volume-based software ANSYS CFX 12.1.

The maximum WSS at the lesion site along with the total area of low WSS in each vessel were measured. On the basis of previous studies, a threshold of <1 Pa was chosen to define low WSS: Samady et al demonstrated greater progression of plaque area, necrotic core, and constrictive remodeling in coronary segments with WSS <1 Pa in a longitudinal intravascular ultrasound study; similarly, Stone et al found coronary segments with WSS <1.2 Pa exhibited plaque progression and constrictive remodeling on serial intravascular ultrasound examinations⁶; lastly, Kumar et al showed a higher prevalence of endothelial dysfunction in coronary segments with WSS <1 Pa.⁷ An example of a coronary artery with CFD-derived WSS color mapping is provided in Figure 1.

Statistical Analysis

Continuous variables were expressed as mean±SD for normally distributed data, and median (interquartile range) for nonnormally distributed data. Categorical variables were expressed as frequencies (percentages). The study cohort was divided into nonobstructive (%DS <50) and obstructive (%DS ≥50) lesions, and the Mann-Whitney *U* test was used to compare differences in the total area of low WSS and maximum lesion WSS between ischemic and nonischemic vessels. Spearman rank correlation was used to assess the relationship between different WSS parameters and coronary physiology indices. Multiple regression analysis was performed with 2 separate models to determine whether the coronary physiology indices independently predicted WSS. Model 1 adjusted for FFR, %DS, and IMR, whereas model 2 adjusted for iFR, %DS, and IMR. Results were expressed as standardized coefficients (β) with 95% CIs. All analyses were performed using SPSS version 23 and Graphpad Prism version 8.4.0. A 2-tailed probability value <0.05 was considered statistically significant.

RESULTS

Baseline Characteristics

A total of 107 vessels from 88 patients were included in this study. The mean age was 63±11 years, and

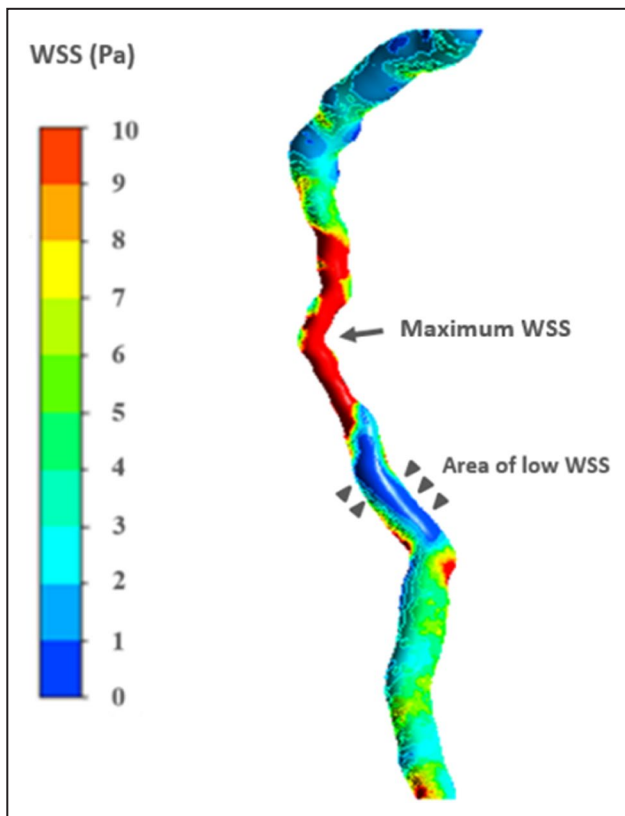


Figure 1. Color-coded wall shear stress (WSS) map of a left anterior descending artery.

Computational fluid dynamics analysis was performed on 3-dimensional reconstructions of coronary arteries. WSS values along the arteries were displayed as color-coded maps. The total area of low WSS (defined as <1 Pa, indicated by the arrowheads) and the maximum lesion WSS (indicated by the arrow) were measured.

28% were women. Most patients had stable coronary artery disease (72%), and the left anterior descending artery was the most commonly studied vessel (70%). The median lesion %DS was 47% (interquartile range, 37%–57%), and median FFR and iFR were 0.85 (interquartile range, 0.73–0.90) and 0.89 (interquartile range, 0.83–0.95), respectively. There were 40 (37%) lesions with $\text{FFR} \leq 0.80$, and 54 (51%) with $\text{iFR} \leq 0.89$. FFR correlated significantly with iFR ($r_s=0.91$; $P<0.001$), whereas IMR did not correlate with FFR ($r_s=0.02$; $P=0.87$) or iFR ($r_s=-0.02$; $P=0.82$). Details of patient comorbidities and lesion characteristics are summarized in Table 1.

Coronary Physiology Indices and Low WSS

Vessels with ischemic FFR and iFR values had larger total area of low WSS compared with nonischemic vessels (FFR: 73 versus 28 mm^2 [$P<0.001$]; iFR: 68 versus 26 mm^2 [$P<0.001$]) (Figure 2A). There was no significant difference in the total area of low WSS

Table 1. Baseline Characteristics

Parameters	Values
Patient, n	88
Vessel, n	107
Age, y	63 \pm 11
Women	25 (28)
Comorbidities	
Diabetes	31 (35)
Hypertension	61 (69)
Hyperlipidemia	61 (69)
Smoker	23 (26)
Clinical presentation	
Stable coronary disease	63 (72)
Unstable angina	14 (16)
NSTEMI	9 (10)
STEMI	2 (2)
Lesion characteristics	
Diameter stenosis, %	47 (37–57)
Target territory	
LAD	76 (71)
LCX	18 (17)
RCA	13 (12)
Coronary physiology indices	
FFR	0.85 (0.73–0.90)
iFR	0.89 (0.83–0.95)
IMR	22 (14–28)

Data are given as number, number (percentage), mean \pm SD, or median (interquartile range). FFR indicates fractional flow reserve; iFR, instantaneous wave-free ratio; IMR, index of microcirculatory resistance; LAD, left anterior descending artery; LCX, left circumflex artery; NSTEMI, non-ST-segment-elevation myocardial infarction (nonculprit vessel interrogated); RCA, right coronary artery; and STEMI, ST-segment-elevation myocardial elevation (nonculprit vessel interrogated).

between vessels with abnormal or normal IMR (63 versus 38 mm^2 ; $P=0.16$).

In vessels with angiographically nonobstructive stenoses (%DS $<50\%$, $n=62$), the total area of low WSS was significantly larger in those with ischemic FFR (63 versus 26 mm^2 ; $P=0.002$) and iFR (53 versus 24 mm^2 ; $P=0.01$) values compared with nonischemic vessels (Figure 2B). Similarly, in vessels with obstructive lesions (%DS $\geq 50\%$, $n=45$), the total area of low WSS was larger in those with ischemic FFR (90 versus 40 mm^2 ; $P=0.01$) and iFR (90 versus 30 mm^2 ; $P<0.001$) values (Figure 2C).

The total area of low WSS correlated significantly with FFR ($r_s=-0.58$; $P<0.001$), iFR ($r_s=-0.64$; $P<0.001$), and %DS ($r_s=0.65$; $P<0.001$), but not with IMR ($r_s=0.09$; $P=0.34$) (Figure 3). In a multiple regression model incorporating FFR, %DS, and IMR, both FFR and %DS were independent predictors of the total area of low WSS (FFR: $\beta=-0.44$; 95% CI, -0.62 to -0.25 ; $P<0.001$; %DS: $\beta=0.34$; 95% CI, 0.16 – 0.53 ;

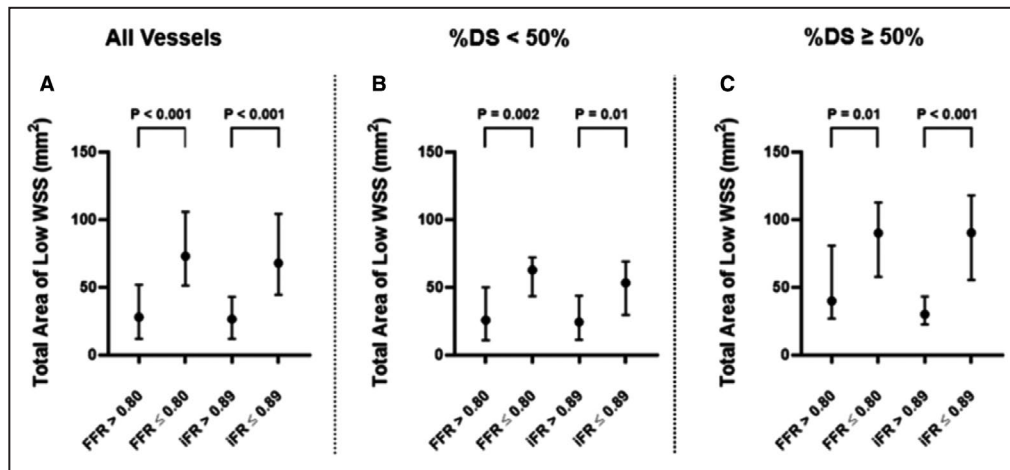


Figure 2. Difference in total area of low wall shear stress (WSS) between ischemic and nonischemic vessels.

A, The difference in total area of low WSS between ischemic and nonischemic vessels in the entire cohort (n=107). **B,** The difference in total area of low WSS between ischemic and nonischemic vessels with angiographically nonobstructive stenoses (n=62). **C,** The difference in total area of low WSS between ischemic and nonischemic vessels with angiographically obstructive stenoses (n=45). The Mann-Whitney *U* test was used to compare differences between groups. %DS indicates percentage diameter stenosis; FFR, fractional flow reserve; and iFR, instantaneous wave-free ratio.

$P < 0.001$) (Table 2). Similarly, after incorporating iFR, %DS, and IMR in a separate model, iFR and %DS were also independent predictors of the total area of low WSS (iFR: $\beta = -0.45$; 95% CI, -0.62 to -0.28 ; $P < 0.001$; %DS: $\beta = 0.37$; 95% CI, 0.20 – 0.54 ; $P < 0.001$) (Table 3). IMR did not predict the total area of low WSS in either model.

Coronary Physiology Indices and High WSS

Vessels with ischemic FFR and iFR values had significantly greater maximum lesion WSS compared with nonischemic vessels (FFR: 95 versus 39 Pa [$P < 0.001$]; iFR: 89 versus 37 Pa [$P < 0.001$]) (Figure 4A). There was no significant difference in maximum lesion WSS between vessels with abnormal or normal IMR.

In vessels with angiographically nonobstructive stenoses, maximum lesion WSS was significantly greater in those with ischemic FFR (90 versus 37 Pa; $P < 0.001$) and iFR (76 versus 28 Pa; $P = 0.002$) values compared with nonischemic vessels (Figure 4B). Similarly, in vessels with obstructive stenoses, maximum lesion WSS was significantly greater in those with ischemic FFR (104 versus 49 Pa; $P = 0.001$) and iFR (103 versus 43 Pa; $P < 0.001$) values (Figure 4C).

Maximum lesion WSS correlated significantly with FFR ($r_s = -0.64$; $P < 0.001$), iFR ($r_s = -0.70$; $P < 0.001$), and %DS ($r_s = 0.66$; $P < 0.001$), but not with IMR ($r_s = 0.07$; $P = 0.49$) (Figure 5). In a multiple regression model incorporating FFR, %DS, and IMR, both FFR and %DS were independent predictors of maximum

lesion WSS (FFR: $\beta = -0.53$; 95% CI, -0.70 to -0.36 ; $P < 0.001$; %DS: $\beta = 0.30$; 95% CI, 0.12 – 0.47 ; $P < 0.001$) (Table 2). Similarly, after incorporating iFR, %DS, and IMR in a separate model, iFR and %DS were also independent predictors of maximum lesion WSS (iFR: $\beta = -0.58$; 95% CI, -0.73 to -0.43 ; $P < 0.001$; %DS: $\beta = 0.31$; 95% CI, 0.16 – 0.45 ; $P < 0.001$) (Table 3). IMR did not predict maximum lesion WSS in either model.

DISCUSSION

To the best of our knowledge, this is the first study to demonstrate a significant independent relationship between ischemia-inducing epicardial coronary stenoses and pathological WSS. On the other hand, we did not find any relationship between microcirculatory dysfunction and pathological WSS. Given the established evidence for low WSS in plaque progression^{5,7,8} and high WSS in vulnerable plaque transformation,^{9,10} our results provide a potential explanation for the higher incidence of adverse events in vessels with functionally significant epicardial coronary stenoses.

Clinical Relevance of Pathological WSS in Coronary Arteries

Despite being a systemic process, atherosclerosis preferentially affects specific regions of the coronary arterial circulation. For example, the culprit lesion in acute myocardial infarction is often located near bifurcations and major curvatures, where increased

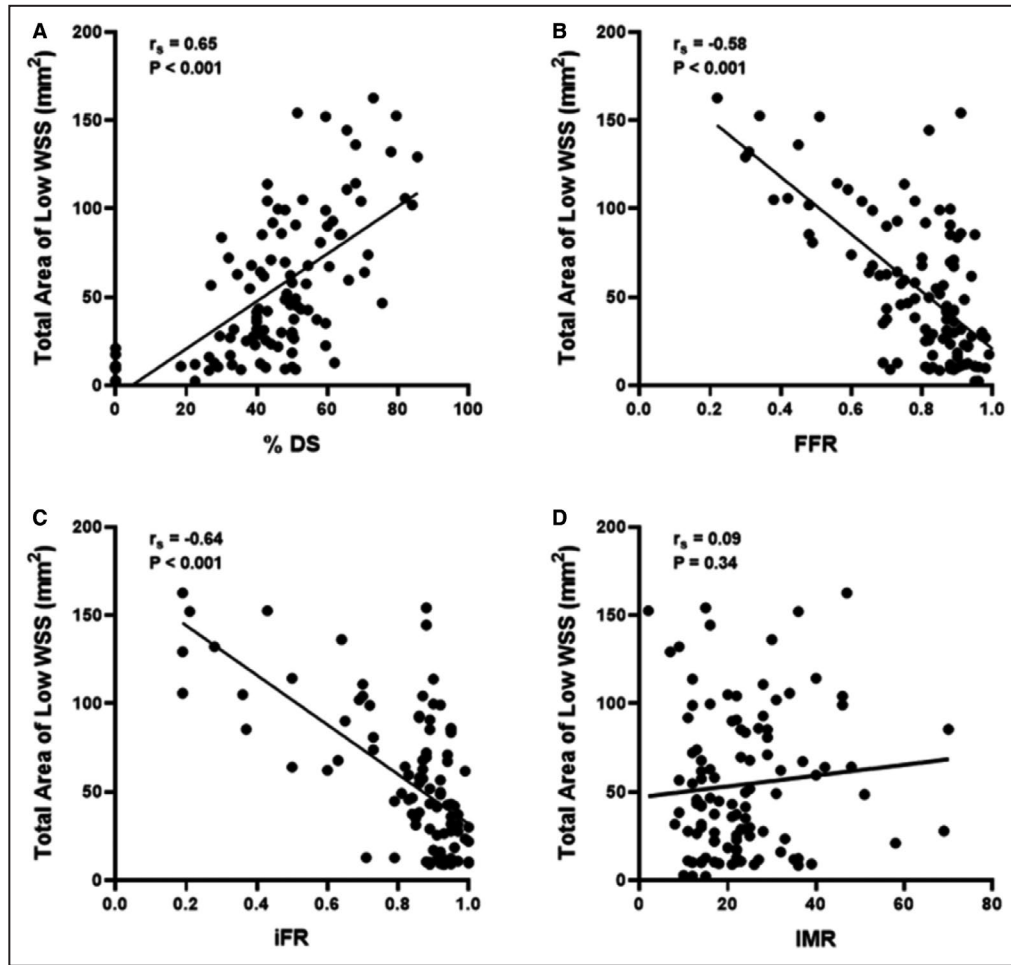


Figure 3. Relationship between total area of low wall shear stress (WSS), fractional flow reserve (FFR), instantaneous wave-free ratio (iFR), percentage diameter stenosis (%DS), and index of microcirculatory resistance (IMR).

Scatterplot and correlation between the total area of low WSS and %DS (A), FFR (B), iFR (C), and IMR (D) (n=107). The total area of low WSS correlated significantly with %DS, FFR, and iFR, and did not correlate with IMR. Spearman rank correlation was used to test for correlation between the variables.

blood flow disturbances occur.²⁰ Studies using CFD analysis have implicated WSS as a potential explanation for this phenomenon. In addition, the presence of a coronary stenosis further modulates local WSS perturbations; high WSS generally occurs at the throat of the lesion, whereas low and oscillatory WSS occurs proximal and distal to the site of maximal stenosis.²¹ Natural history studies of WSS in human coronary arteries demonstrated that coronary segments

with low WSS, variably defined as <1 to 1.2 Pa, were associated with plaque progression, constrictive remodeling, and necrotic core development.^{5,6,8} This phenomenon was postulated to be secondary to endothelial activation of the protein kinase and nuclear factor-κB signaling pathways in response to low WSS, with subsequent expression of proinflammatory and apoptotic genes.^{22,23} Furthermore, coronary segments with low WSS have been shown to be

Table 2. Multiple Regression Model Adjusted for %DS, FFR, and IMR

WSS parameters	%DS			FFR			IMR		
	β	95% CI	P value	β	95% CI	P value	β	95% CI	P value
ALWSS, mm ²	0.34	0.16 to 0.53	<0.001	-0.44	-0.62 to -0.25	<0.001	0.02	-0.12 to 0.16	0.79
Maximum WSS, Pa	0.30	0.12 to 0.47	0.001	-0.53	-0.70 to -0.36	<0.001	0.05	-0.08 to 0.17	0.47

ALWSS indicates area of low WSS; %DS, percentage diameter stenosis; FFR, fractional flow reserve; IMR, index of microcirculatory resistance; and WSS, wall shear stress.

Table 3. Multiple Regression Model Adjusted for %DS, iFR, and IMR

WSS parameters	%DS			iFR			IMR		
	β	95% CI	P value	β	95% CI	P value	β	95% CI	P value
ALWSS, mm ²	0.37	0.20 to 0.54	<0.001	-0.45	-0.62 to -0.28	<0.001	-0.06	-0.16 to 0.12	0.77
Maximum WSS, Pa	0.31	0.16 to 0.45	<0.001	-0.58	-0.73 to -0.43	<0.001	-0.00	-0.12 to 0.11	0.95

ALWSS indicates area of low WSS; %DS, percentage diameter stenosis; iFR, instantaneous wave-free ratio; IMR, index of microcirculatory resistance; and WSS, wall shear stress.

associated with endothelial dysfunction, a precursor to the development of atherosclerosis.^{7,24} Therefore, it is evident that low WSS leads to atherosclerosis progression and endothelial dysfunction in the coronary arteries.

Apart from low WSS, abnormally high WSS within coronary lesions also carries deleterious effects. A serial virtual histological intravascular ultrasound study has shown that high WSS induced excessive expansive remodeling with greater necrotic core and calcium progression, leading to the development of vulnerable plaques.⁵ More importantly, high WSS has been found to be associated with adverse clinical outcomes. In a subgroup analysis of the Fractional Flow Reserve versus Angiography for Multivessel Evaluation (FAME) II study, Kumar et al identified high WSS in the proximal-lesion segment to be an independent predictor of future myocardial infarction in un-revascularized patients.⁹ In a separate study utilizing computed tomography coronary angiography, Lee et al identified coronary lesions with high WSS to be a significant predictor of future acute coronary syndrome (Please

insert reference 10 here : Lee et al. JACC Cardiovasc Imaging. 2019 Jun;12(6):1032-1043)

FFR and iFR Independently Predicted Burden of Low WSS and Maximum Lesion WSS

Our finding of a significant relationship between abnormal FFR/iFR and pathological WSS provide a potential explanation for the could be explained as follows: by virtue of Ohm's law, the pressure gradient (voltage) between the guide catheter and distal pressure sensor is influenced by the amount of flow (current) and stenosis severity (resistance). In the setting of lesions with identical stenosis severity, a vessel supplying a larger amount of myocardium has proportionally larger flow and higher pressure gradient (ie, lower FFR/iFR). This leads to increased flow velocity, Reynold's number ($[\text{velocity} \times \text{lumen diameter}] / \text{viscosity}$), and flow reattachment length,²¹ resulting in both higher maximum lesion WSS and a larger area of flow recirculation zone with low and oscillating WSS (Figure 6). Furthermore, FFR

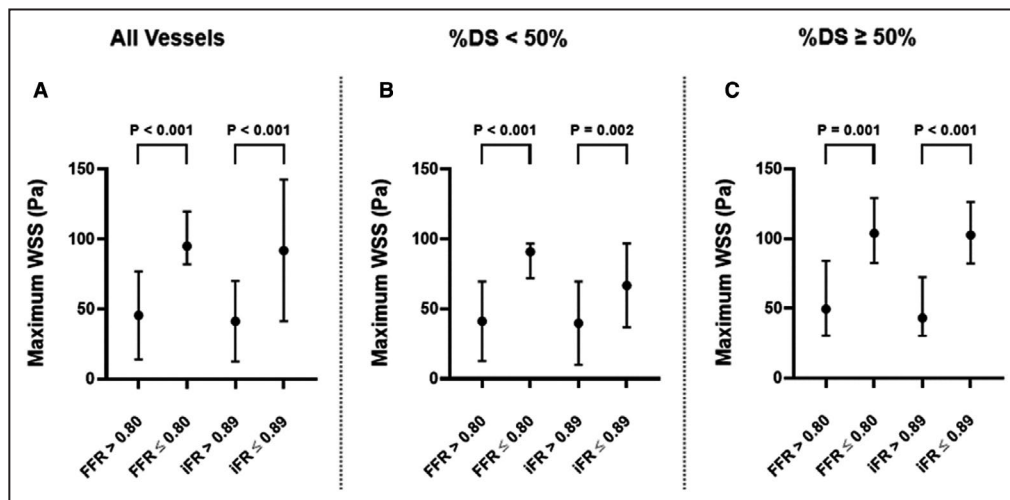


Figure 4. Difference in maximum lesion wall shear stress (WSS) between ischemic and nonischemic vessels.

A, The difference in maximum lesion WSS between ischemic and nonischemic vessels in the entire cohort (n=107). **B**, The difference in maximum lesion WSS between ischemic and nonischemic vessels with angiographically nonobstructive stenoses (n=62). **C**, The difference in maximum lesion WSS between ischemic and nonischemic vessels with angiographically obstructive stenoses (n=45). The Mann-Whitney U test was used to compare differences between groups. %DS indicates percentage diameter stenosis; FFR, fractional flow reserve; and iFR, instantaneous wave-free ratio.

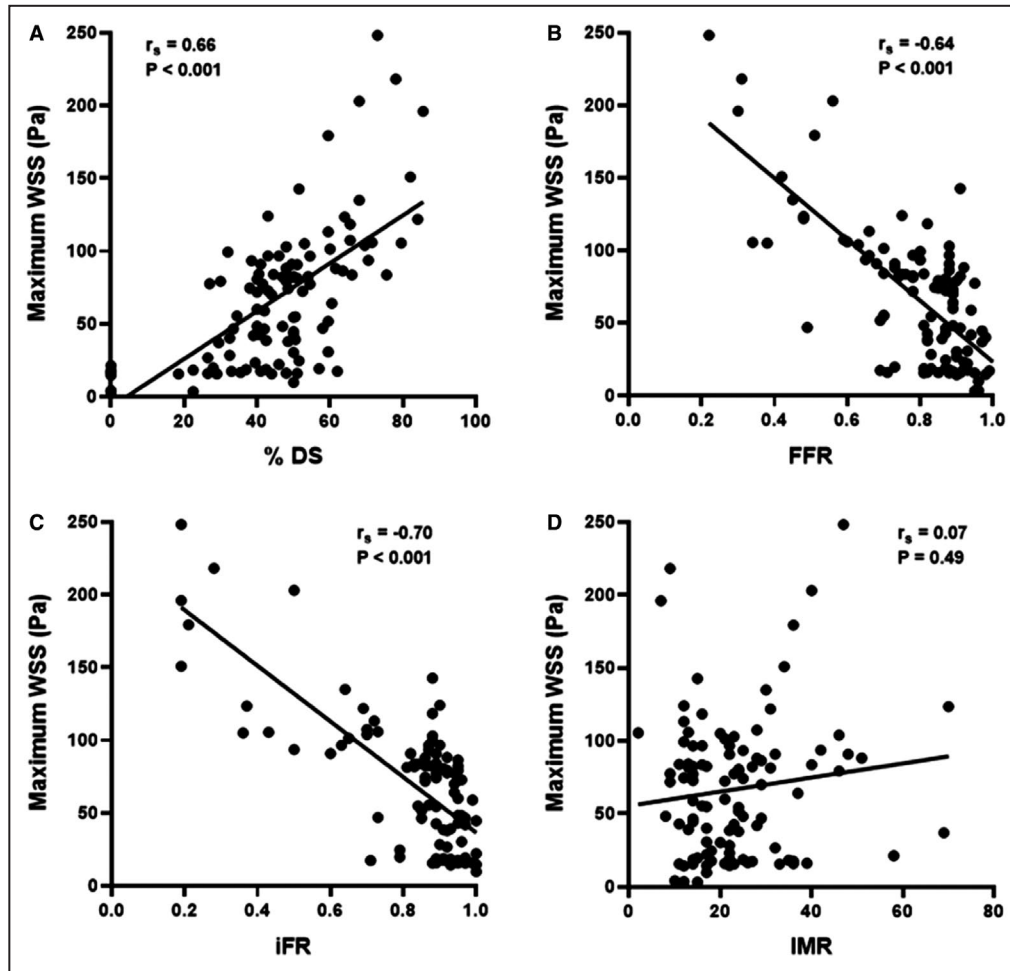


Figure 5. Relationship between maximum lesion wall shear stress (WSS), fractional flow reserve (FFR), instantaneous wave-free ratio (iFR), percentage diameter stenosis (%DS), and index of microcirculatory resistance (IMR).

Scatterplot and correlation between the maximum lesion WSS and %DS (A), FFR (B), iFR (C), and IMR (D) ($n=107$). Maximum lesion WSS correlated significantly with %DS, FFR, and iFR, and did not correlate with IMR. Spearman rank correlation was used to test for correlation between the variables.

and iFR are summation indexes that assess the cumulative effect of atherosclerotic disease in the epicardial compartment of the coronary circulation by measuring the total pressure loss along the interrogated length of vessel. This allows integrated assessment of the effects of diffuse disease beyond the main lesion, a common and important contributor to myocardial ischemia.²⁵ The presence of diffuse disease upstream or downstream to the main lesion has the potential to further modulate the local WSS milieu, and may explain the additive value of FFR and iFR over an idealized model of isolated focal stenosis in predicting WSS changes.

Although FFR and iFR both evaluate the epicardial component of the coronary circulation, there are distinct differences between the two tests that account for the 10% to 30% discordance rates observed in previous studies.²⁶ FFR measures the distal/proximal pressure ratio during pharmacologically induced

hyperemia, a state in which the microcirculatory resistance is minimized;²⁷ whereas iFR measures the distal/proximal pressure ratio during the diastolic wave-free period at rest, a state that is significantly influenced by the additional effects of coronary autoregulation.²⁸ Therefore, there may be differences between FFR and iFR in their ability to predict WSS. In our study, both ischemic FFR and iFR values were significantly associated with pathological WSS; further studies comparing resting and hyperemic shear stress may be helpful to evaluate the differences between the two tests.

Clinical Implications: A Potential Explanation for the Prognostic Impact of Myocardial Ischemia

Observational studies involving treadmill and myocardial perfusion stress have demonstrated an association

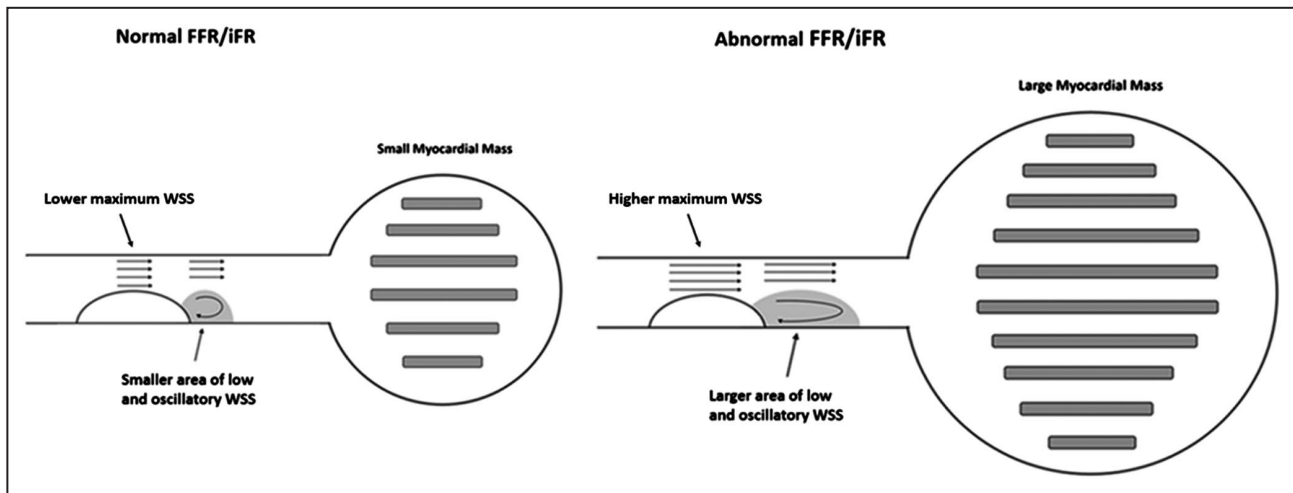


Figure 6. Influence of myocardial mass on the epicardial physiological indexes and pathological wall shear stress (WSS).

Figure 6 illustrates the impact of myocardial mass on fractional flow reserve/instantaneous wave-free ratio, maximum lesion WSS, and the area of low WSS in the presence of coronary lesions with identical severity (50% stenosis in this illustration). By virtue of Ohm's law, a larger myocardial mass subtended by an artery has comparatively higher flow and a higher pressure gradient, despite identical lesion stenosis geometry. The increased flow corresponds to a proportional increase in flow velocity and the reattachment length of the flow recirculation zone, leading to greater maximum lesion WSS and a larger area of low and oscillatory WSS. FFR indicates fractional flow reserve; and iFR, instantaneous wave-free ratio.

between ischemia severity and clinical outcomes in patients with stable coronary artery disease.^{1,29} The advent of FFR has further enabled localization of ischemia-inducing coronary lesions, thus influencing treatment decisions in multivessel disease. The FAME study demonstrated superiority of FFR-guided percutaneous coronary intervention over angiography-guided percutaneous coronary intervention, while the FAME II study showed increased clinical events in patients with FFR ≤ 0.80 randomized to medical therapy. Collectively, studies to date have established myocardial ischemia to be an important prognostic factor. Yet, the pathophysiological mechanism underpinning this phenomenon has not been clearly elucidated. Our results provide a potential explanation for the additive prognostic impact of ischemia over angiographic severity alone, by demonstrating a significant relationship between ischemic FFR/iFR and pathological WSS that persisted after adjusting for lesion stenosis severity. Future studies to investigate whether percutaneous coronary intervention or novel drug therapies, such as those that specifically target shear-dependent von Willebrand factor–glycoprotein Ib receptor ligand interaction, could improve clinical outcomes in lesion subsets exhibiting pathological WSS would help further our fundamental understanding of WSS and its impact in coronary artery disease.³⁰

Study Limitations

There are several limitations to this study. First, the CFD analysis was performed in 3-D reconstructed vessels from angiographic rather than optical coherence

tomography or intravascular ultrasound images, which would have provided superior spatial resolution. Furthermore, our CFD model did not include branching vessels, which potentially reduces the accuracy of WSS values around side branches and bifurcations. However, the accuracy of our modeling was increased by incorporating directly measured physiological parameters as boundary conditions. Our method of angiographic WSS has been well validated previously by our group and others.^{7,9,18,19} Second, our study was not designed to assess how WSS and coronary physiology indices affected outcomes, as most patients with pathological WSS and ischemia-inducing lesions underwent subsequent revascularization. Third, our study did not examine how intervention to ischemic lesions modifies WSS perturbations, and further studies are needed in future to address this question.

CONCLUSIONS

FFR and iFR predicted pathological low and high WSS within coronary arteries, irrespective of the angiographic severity of the underlying lesion. No relationship was found between microcirculatory dysfunction and pathological WSS.

ARTICLE INFORMATION

Received August 3, 2021; accepted December 6, 2021.

Affiliations

Department of Cardiology, Concord Hospital (C.C.Y.W., A.J., C.A., L.K., A.S.C.Y.), Department of Cardiology, Royal North Shore Hospital (R.B.) and

Department of Cardiology, Royal Prince Alfred Hospital (M.K.C.N.), University of Sydney, Australia; Faculty of Medicine and Health Sciences, Macquarie University, Sydney, Australia (A.J., A.S.C.Y.); Department of Cardiology, Royal Adelaide Hospital, University of Adelaide, Australia (J.K.L.); and Division of Cardiovascular Medicine, Stanford University, Stanford, CA (W.F.F.).

Acknowledgments

We would like to thank Mr Johan Svanerud (Coroventis Research AB, Uppsala, Sweden) for assistance with the Coroflow system; and Prof Itsu Sen (Faculty of Medicine and Health Sciences, Macquarie University, Sydney, Australia) for critical review of the manuscript.

Sources of Funding

This work was supported by a Postgraduate Health Professional Scholarship from the National Heart Foundation of Australia (award number 102332).

Disclosures

Dr Yong has received minor honoraria and research support from Abbott and Philips Healthcare. Dr Fearon has received research support from Abbott and Medtronic; and has minor stock options with HeartFlow. Dr Ng has received research support from Abbott. The remaining authors have nothing to disclose.

REFERENCES

- Hachamovitch R, Berman DS, Shaw LJ, Kiat H, Cohen I, Cabico JA, Friedman J, Diamond GA. Incremental prognostic value of myocardial perfusion single photon emission computed tomography for the prediction of cardiac death: differential stratification for risk of cardiac death and myocardial infarction. *Circulation*. 1998;97:535–543. doi: 10.1161/01.CIR.97.6.535
- Zimmermann FM, Ferrara A, Johnson NP, van Nunen LX, Escaned J, Albertsson P, Erbel R, Legrand V, Gwon HC, Remkes WS, et al. Deferral vs. performance of percutaneous coronary intervention of functionally non-significant coronary stenosis: 15-year follow-up of the DEFER trial. *Eur Heart J*. 2015;36:3182–3188. doi: 10.1093/eurheartj/ehv452
- Tonino PAL, De Bruyne B, Pijls NHJ, Siebert U, Ikeno F, van t Veer M, Klauss V, Manoharan G, Engström T, Oldroyd KG, et al. Fractional flow reserve versus angiography for guiding percutaneous coronary intervention. *N Engl J Med*. 2009;360:213–224. doi: 10.1056/NEJMo a0807611
- Lee JM, Jung JH, Hwang D, Park J, Fan Y, Na SH, Doh JH, Nam CW, Shin ES, Koo BK. Coronary flow reserve and microcirculatory resistance in patients with intermediate coronary stenosis. *J Am Coll Cardiol*. 2016;67:1158–1169. doi: 10.1016/j.jacc.2015.12.053
- Samady H, Eshtehardi P, McDaniel MC, Suo J, Dhawan SS, Maynard C, Timmins LH, Quyyumi AA, Giddens DP. Coronary artery wall shear stress is associated with progression and transformation of atherosclerotic plaque and arterial remodeling in patients with coronary artery disease. *Circulation*. 2011;124:779–788. doi: 10.1161/CIRCULATIONAHA.111.021824
- Stone PH, Coskun AU, Kinlay S, Popma JJ, Sonka M, Wahle A, Yeghiazarians Y, Maynard C, Kuntz RE, Feldman CL. Regions of low endothelial shear stress are the sites where coronary plaque progresses and vascular remodelling occurs in humans: an in vivo serial study. *Eur Heart J*. 2007;28:705–710. doi: 10.1093/eurheartj/ehl575
- Kumar A, Hung OY, Piccinelli M, Eshtehardi P, Corban MT, Sternheim D, Yang B, Lefieux A, Molony DS, Thompson EW, et al. Low coronary wall shear stress is associated with severe endothelial dysfunction in patients with nonobstructive coronary artery disease. *JACC Cardiovasc Interv*. 2018;11:2072–2080. doi: 10.1016/j.jcin.2018.07.004
- Stone PH, Saito S, Takahashi S, Makita Y, Nakamura S, Kawasaki T, Takahashi A, Katsuki T, Nakamura S, Namiki A, et al. Prediction of progression of coronary artery disease and clinical outcomes using vascular profiling of endothelial shear stress and arterial plaque characteristics: the PREDICTION Study. *Circulation*. 2012;126:172–181. doi: 10.1161/CIRCULATIONAHA.112.096438
- Kumar A, Thompson EW, Lefieux A, Molony DS, Davis EL, Chand N, Fournier S, Lee HS, Suh J, Sato K, et al. High coronary shear stress in patients with coronary artery disease predicts myocardial infarction. *J Am Coll Cardiol*. 2018;72:1926–1935. doi: 10.1016/j.jacc.2018.07.075
- Lee JM, Choi G, Koo BK, Hwang D, Park J, Zhang J, Kim KJ, Tong Y, Kim HJ, Grady L, et al. Identification of high-risk plaques destined to cause acute coronary syndrome using coronary computed tomographic angiography and computational fluid dynamics. *JACC Cardiovasc Imaging*. 2019;12:1032–1043. doi: 10.1016/j.jcmg.2018.01.023
- Yong AS, Layland J, Fearon WF, Ho M, Shah MG, Daniels D, Whitbourn R, MacIsaac A, Kritharides L, Wilson A, et al. Calculation of the index of microcirculatory resistance without coronary wedge pressure measurement in the presence of epicardial stenosis. *JACC Cardiovasc Interv*. 2013;6:53–58. doi: 10.1016/j.jcin.2012.08.019
- Lau JK, Roy P, Javadzadegan A, Moshfegh A, Fearon WF, Ng M, Lowe H, Brieger D, Kritharides L, Yong AS. Remote ischemic preconditioning acutely improves coronary microcirculatory function. *J Am Heart Assoc*. 2018;7:e009058. doi: 10.1161/JAHA.118.009058
- Lee JM, Layland J, Jung JH, Lee HJ, Echavarría-Pinto M, Watkins S, Yong AS, Doh JH, Nam CW, Shin ES, et al. Integrated physiologic assessment of ischemic heart disease in real-world practice using index of microcirculatory resistance and fractional flow reserve: insights from the International Index of Microcirculatory Resistance Registry. *Circ Cardiovasc Interv*. 2015;8:e002857. doi: 10.1161/CIRCINTERVENTIONS.115.002857
- Johnson NP, Li W, Chen X, Hennigan B, Watkins S, Berry C, Fearon WF, Oldroyd KG. Diastolic pressure ratio: new approach and validation vs. the instantaneous wave-free ratio. *Eur Heart J*. 2019;40:2585–2594. doi: 10.1093/eurheartj/ehz230
- Svanerud J, Ahn J-M, Jeremias A, van 't Veer M, Gore A, Maehara A, Crowley A, Pijls NHJ, De Bruyne B, Johnson NP, et al. Validation of a novel non-hyperaemic index of coronary artery stenosis severity: the Resting Full-cycle Ratio (VALIDATE RFR) study. *EuroIntervention*. 2018;14:806–814. doi: 10.4244/EIJ-D-18-00342
- Van't Veer M, Pijls NHJ, Hennigan B, Watkins S, Ali ZA, De Bruyne B, Zimmermann FM, van Nunen LX, Barbato E, Berry C, et al. Comparison of different diastolic resting indexes to iFR: are they all equal? *J Am Coll Cardiol*. 2017;70:3088–3096. doi: 10.1016/j.jacc.2017.10.066
- Yong AS, Ng AC, Brieger D, Lowe HC, Ng MK, Kritharides L. Three-dimensional and two-dimensional quantitative coronary angiography, and their prediction of reduced fractional flow reserve. *Eur Heart J*. 2011;32:345–353. doi: 10.1093/eurheartj/ehq259
- Javadzadegan A, Yong AS, Chang M, Ng AC, Yiannikas J, Ng MK, Behnia M, Kritharides L. Flow recirculation zone length and shear rate are differentially affected by stenosis severity in human coronary arteries. *Am J Physiol Heart Circ Physiol*. 2013;304:H559–H566. doi: 10.1152/ajpheart.00428.2012
- Javadzadegan A, Moshfegh A, Qian Y, Ng MK, Kritharides L, Yong AS. The relationship between coronary lesion characteristics and pathologic shear in human coronary arteries. *Clin Biomech*. 2018;60:177–184. doi: 10.1016/j.clinbiomech.2018.10.023
- McDaniel MC, Galbraith EM, Jeroudi AM, Kashtan OR, Eshtehardi P, Suo J, Dhawan S, Voeltz M, Devireddy C, Oshinski J, et al. Localization of culprit lesions in coronary arteries of patients with ST-segment elevation myocardial infarctions: relation to bifurcations and curvatures. *Am Heart J*. 2011;161:508–515. doi: 10.1016/j.ahj.2010.11.005
- Gijsen FJ, van de Vosse FN, Janssen JD. Wall shear stress in backward-facing step flow of a red blood cell suspension. *Biorheology*. 1998;35:263–279. doi: 10.1016/S0006-355X(99)80010-9
- Hung OY, Brown AJ, Ahn SG, Veneziani A, Giddens DP, Samady H. Association of wall shear stress with coronary plaque progression and transformation. *Interv Cardiol Clin*. 2015;4:491–502. doi: 10.1016/j.iccl.2015.06.009
- Cecchi E, Giglioli C, Valente S, Lazzeri C, Gensini GF, Abbate R, Mannini L. Role of hemodynamic shear stress in cardiovascular disease. *Atherosclerosis*. 2011;214:249–256. doi: 10.1016/j.atherosclerosis.2010.09.008
- Puri R, Leong DP, Nicholls SJ, Liew GYL, Nelson AJ, Carbone A, Copus B, Wong DT, Beltrame JF, Worthley SG, et al. Coronary artery wall shear stress is associated with endothelial dysfunction and expansive arterial remodeling in patients with coronary artery disease. *EuroIntervention*. 2015;10:1440–1448. doi: 10.4244/EIJV10I12A249
- De Bruyne B, Hersbach F, Pijls NH, Bartunek J, Bech JW, Heyndrickx GR, Gould KL, Wijns W. Abnormal epicardial coronary resistance in patients with diffuse atherosclerosis but "normal" coronary angiography. *Circulation*. 2001;104:2401–2406. doi: 10.1161/hc4501.099316
- Lee JM, Doh JH, Nam CW, Shin ES, Koo BK. Functional approach for coronary artery disease: filling the gap between evidence and practice. *Korean Circ J*. 2018;48:179–190. doi: 10.4070/kcj.2017.0393

-
27. Pijls NH, De Bruyne B, Peels K, Van Der Voort PH, Bonnier HJ, Bartunek JKJJ, Koolen JJ. Measurement of fractional flow reserve to assess the functional severity of coronary-artery stenoses. *N Engl J Med*. 1996;334:1703–1708. doi: 10.1056/NEJM199606273342604
 28. de Waard GA, Cook CM, van Royen N, Davies JE. Coronary autoregulation and assessment of stenosis severity without pharmacological vasodilation. *Eur Heart J*. 2018;39:4062–4071. doi: 10.1093/eurheartj/ehx669
 29. Morrow K, Morris CK, Froelicher VF, Hideg A, Hunter D, Johnson E, Kawaguchi T, Lehmann K, Ribisl PM, Thomas R, et al. Prediction of cardiovascular death in men undergoing noninvasive evaluation for coronary artery disease. *Ann Intern Med*. 1993;118:689–695. doi: 10.7326/0003-4819-118-9-199305010-00005
 30. Rana A, Westein E, Niego B, Hagemeyer CE. Shear-dependent platelet aggregation: mechanisms and therapeutic opportunities. *Front Cardiovasc Med*. 2019;6:141. doi: 10.3389/fcvm.2019.00141